Unc-45 Mutations in *Caenorhabditis elegans* Implicate a CRO1/She4p-like Domain in Myosin Assembly

José M. Barral,* Christopher C. Bauer,‡ Irving Ortiz,‡ and Henry F. Epstein*‡

*Department of Biochemistry and ‡Department of Neurology, Baylor College of Medicine, Houston, Texas 77030

Abstract. The *Caenorhabditis elegans unc-45* locus has been proposed to encode a protein machine for myosin assembly. The UNC-45 protein is predicted to contain an NH_2-terminal domain with three tetratricopeptide repeat motifs, a unique central region, and a COOH-terminal domain homologous to CRO1 and She4p. CRO1 and She4p are fungal proteins required for the segregation of other molecules in budding, endocytosis, and septation. Three mutations that lead to temperature-sensitive (*ts*) alleles have been localized to conserved residues within the CRO1/She4p-like domain, and two lethal alleles were found to result from stop codon mutations in the central region that would prevent translation of the COOH-terminal domain. Electron microscopy shows that thick filament accumulation in vivo is decreased by ~50% in the CB286 *ts* mutant grown at the restrictive temperature. The thick filaments that assemble have abnormal structure. Immunofluorescence and immunoelectron microscopy show that myosins A and B are scrambled, in contrast to their assembly into distinct regions at the permissive temperature and in wild type. This abnormal structure correlates with the high degree of instability of the filaments in vitro as reflected by their extremely low yields and shortened lengths upon isolation. These results implicate the UNC-45 CRO1/She4p-like region in the assembly of myosin isoforms in *C. elegans* and suggest a possible common mechanism for the function of this UCS (UNC-45/CRO1/She4p) protein family.

Key words: myosin • muscle • chaperone • biosynthesis • *Caenorhabditis elegans*

THE localization of molecules to distinct regions within cells is a critical process in the establishment of cell polarity and cellular differentiation. Although the mechanisms and molecules responsible for these processes are incompletely known, considerable evidence points towards the cytoskeleton and its associated motor proteins as key players in the generation of cellular diversity. Studies seeking to understand the mechanisms underlying the differential segregation of determinants between mother and daughter cells in *Saccharomyces cerevisiae* discovered the protein She4p (Swi5p-dependent *HO* expression; Jansen et al., 1996). She4p and other *SHE* proteins, including the unconventional (class V) myosin Myo4p (She1p), are specifically required for the expression of the *HO* endonuclease in mother, but not daughter, cells. It has been hypothesized that these proteins are involved in the transport of the repressor Ash1p from mother cells to their buds, and thus help to establish a cellular difference in cells that are exposed to identical environmental conditions. She4p was independently found in a genetic screen seeking mutants with defects in endocytosis (Wendland et al., 1996). Beside their defect in the internalization of both bulk lipid and α-factor, *she4-Δ* cells displayed a loss of polarity of actin localization. CRO1, a protein homologous to She4p was found to be involved in the transition between the syncytial and cellular states of the filamentous fungus *Podospora anserina* (Berteaux-Lecellier et al., 1998).

We report here that mutations in a domain homologous to CRO1/She4p in the *Caenorhabditis elegans* protein UNC-45 disrupt myosin assembly in the thick filaments of body wall muscle cells. The structure of *C. elegans* thick filaments is known in considerable detail through the combination of genetic, biochemical and ultrastructural approaches. The thick filaments are bipolar tubular assemblies. They contain an inner core composed of paramyosin and the recently identified filagenins (Epstein et al., 1995; Liu et al., 1998). The outer layer contains two myosin isoforms, A and B, which are differentially localized along the length of the filament (Miller et al., 1983). Myosin A is restricted to a central 1.8-μm-long region, whereas myosin B is present at the 4.4-μm polar regions, but excluded from the central region. Two 0.45-μm zones contain both isoforms at either side of the central region.

Address all correspondence to Dr. Henry F. Epstein, Department of Neurology, Baylor College of Medicine, One Baylor Plaza, Houston, TX 77030. Tel.: (713) 798-4629. Fax: (713) 798-3771. E-mail: hepstein@bcm.tmc.edu

The *unc-45* gene has been proposed to encode an activity necessary for the assembly of myosin into thick filaments (Epstein and Thomson, 1974). Three kinds of alleles have been described, based on their phenotypes: temperature sensitive (*ts*)[1], constitutive lethal (*let*), and maternally rescuable lethal (*mr*; Epstein and Thomson, 1974; Venolia and Waterston, 1990). Strains carrying *ts* alleles display an Unc (uncoordinated or paralyzed) phenotype when grown at the restrictive temperature (25°C), with marked myofibrillar disorganization and diminished accumulation of thick filaments. This temperature-dependent phenotype is reversible, but only during the developmental stages of the organism. Larvae that hatch at the permissive temperature (15°C) have a wild-type phenotype, but develop into Unc adults if switched to 25°C. The converse is also true. However, once the worms have reached adulthood, switching temperature has no effect on the phenotype. Heterozygous strains carrying lethal alleles lead to F$_1$ arrest at the twofold stage of embryonic development, a stage at which loss-of-function mutants in other essential genes that affect myofibril development also cause arrest (Barstead and Waterston, 1991; Williams and Waterston, 1994), including the mhc A gene *myo-3* (Waterston, 1989). Heterozygous strains carrying the *mr* allele lead to viable, but Unc, F$_1$ progeny. These worms, in turn, produce F$_2$ eggs that arrest at the twofold stage. Functional interactions of *unc-45* with myosins A and B have been described, based on the suppression or enhancement of the different *unc-45* phenotypes in strains carrying mutations in the genes of these body wall mhc isoforms (Waterston, 1988; Venolia and Waterston, 1990).

Our analysis of the predicted *unc-45* sequence and the characterization of its genetic alterations demonstrate that the CRO1/She4p-like domain of UNC-45 is the primary target of the different types of mutations studied. Our studies on the in vivo accumulation of thick filaments and body wall mhc isoform content demonstrate that the number of thick filaments and myosin heavy chain (mhc) B content in strain CB286 grown at 25°C is decreased with respect to its 15°C counterpart. We have investigated the nature of the molecular alterations in filaments isolated from the 25°C strain and show that these consist of myosin isoform scrambling. Here we report that these mutant filaments are highly unstable in vitro, as evidenced by their significant decrease in length and number after isolation. These results are consistent with UNC-45 playing a role as a myosin assemblase (Liu et al., 1997) in the construction of body wall thick filaments.

Materials and Methods

Nematode Growth

Nematode strains to be used for obtaining genomic DNA to serve as template for PCR were grown on nematode growth medium plates with

Escherichia coli OP50 (Brenner, 1974) at 15°C (*unc-45 ts* alleles *e286*, *r450*, *su2002*, *b131*, and *m94*), 20°C (wild-type strain N2), or 25°C (*unc-45* lethal alleles *st601* and *st603*). For analysis of muscle structure, SDS-PAGE and isolation of thick filaments, CB286 nematodes were synchronized by seeding eggs obtained by standard methods (Lewis and Fleming, 1995) on peptone enriched plates with *Escherichia coli* NA22 (Schachat et al., 1978) and grown at 15°C (permissive temperature) or 25°C (restrictive temperature). The nematodes were harvested after 72 h of growth at 15°C or 48 h of growth at 25°C, times that corresponded to similar stages of development (young adult).

Sequence Analysis

The predicted *unc-45* sequence was obtained from the *C. elegans* Genome Sequencing Project (The Sanger Centre, Hinxton Hall, Cambridge, UK, and the Washington University School of Medicine, St. Louis, MO). The similarity searches and multiple sequence alignments were performed over the World Wide Web with the Baylor College of Medicine Search Launcher (Smith et al., 1996). The predicted UNC-45 tetratricopeptide repeat (TPR) sequence was modeled to the three-dimensional structure of the human protein phosphatase 5 TPR domain (Das et al., 1998) using the SWISS-MODEL program (Guex and Peitsch, 1997).

cDNA Sequencing

A partial cDNA clone, yk44f2, starting from nucleotide number 820 and ending at the polyadenylation site, was obtained from Dr. Yuji Kohara (Gene Network Laboratory, National Institute of Genetics, Mishima, Japan). The 5′ end of the *unc-45* gene was obtained by screening a stage-specific phage lambda library of embryonic cDNAs obtained from Dr. Peter Okkema (University of Illinois, Chicago, IL). Two primers were constructed: (*a*) Upstream primer Unc45GstUp 5′GAA GAT CTC CCA TGG TTG CTC GAG TAC AGA CTG CGG AGG3′ and (*b*) downstream primer Unc45-2Ddn 5′CCG TCC TCG AAG ATC TTC GTA CTC AGC3′. Primer Unc45GstUp contained the *C. elegans* Genome Sequencing Project predicted *unc-45* start codon and a unique BglII restriction endonuclease recognition site. Primer Unc45-2Ddn was designed to hybridize within the sequence covered by clone yk44f2. A unique ClaI site was present in the overlapping sequences. Long range PCR, using *Taq* Extender PCR Additive (Stratagene, La Jolla, CA) and *Taq* DNA Polymerase (Promega Corp., Madison, WI), was performed with an aliquot of the Okemma library as template. The expected 1.8-kbp product was obtained and digested with BglII and ClaI. Clone yk44f2 was digested with ClaI and a full-length *unc-45* cDNA was obtained by joining these two fragments at the ClaI site. *Exo* 3 DNA exonuclease progressive deletion clones were obtained, following the Erase-a-Base protocol (Promega Corp.), and sequenced by the Molecular Genetics Core Facility of the University of Texas Houston Health Sciences Center (Houston, TX). Further PCR experiments searching for translation start sites upstream of the predicted start site, using primers (*a*) Unc45Exup 5′TGC CCC ATG GAG ATC TAT GAA ACG GCG ACT CGG CAA C3′ and (*b*) Unc45Exdn 5′CCC TCG TCG CGG ATC TCC TCC GC3′ did not yield any PCR products.

Chemical Cleavage of Mismatches

Genomic DNA to serve as template for PCR was obtained from each strain by phenol/chloroform extraction followed by ethanol precipitation using disposable materials only, essentially as described (Sambrook et al., 1989). The following pairs of primers were used to amplify every exon from each strain: (*a*) exons 1, 2, and 3: Set1A, 5′GTC TGC GCT TCA CAC TCT CTA ACA CG3′; Set1B, 5′CAG TTT CGG GAG GTT GGG TCT GC3′; (*b*) exons 4 and 5: Set2A, 5′GCA GAC CCA AGA TTT TCT CAC3′; Set2B, 5′CGA ATG GAA CAA GTG CGC CCT GG3′; (*c*) exon 6: Set3A, 5′GCT ACA ACG AGA AAA CC3′; Set3B, 5′CCG ATT TCC TTG TTC CGT AC3′; (*d*) exon 7: Set4A, 5′CAG ACG CGG CGA TAT GTC TGC3′; Set4B, 5′CCA TTC TTT TCA GCA TGC CCC3′; (*e*) exon 8: Set5A, 5′CAC ACC TCT CTA TTA GAA GGA CG3′; Set5B, 5′GCA GAC CCA TGA ACT GAC AAT CAC TC3′; (*f*) exon 9: Set6A, 5′CGG CAA TTT TCA TTC CTA CGT G3′; Set6B, 5′GCT CTC CAC TCG ATA CTT GTT CGC3′; (*g*) exon 10: Set7A, 5′GGT GTG CGT CTG CAA AAA CG3′; Set7B, 5′GGC GCT TGT GTT GTG AGT CTA TC3′; (*h*) exon 11: Set8A, 5′CGG AAC AAC TGG ACA TCC C3′; Set8B, 5′CGA AAC TTT GAA GCC ACG TGG3′. Chemical cleavage of mismatch (CCM) reactions were carried out as described (Cotton et al.,

---

1988), screening every PCR product from each strain. In brief, wild-type PCR product was labeled with polynucleotide kinase (Boehringer Mannheim Corp., Indianapolis, IN) and allowed to form a heteroduplex with the corresponding unlabeled PCR product from the mutant being screened. The heteroduplex was subjected to hydroxylamine (2.3 M for 2 h at 37°C) or osmium tetroxide (0.025% + 3% pyridine for 1 h at 37°C) modification, followed by piperidine cleavage (10% for 30 min at 90°C). The reactions were separated on an 8% denaturing polyacrylamide gel and autoradiographed. PCR products that showed cleavage products were sequenced by the Molecular Genetics Core Facility of the University of Texas Houston Health Sciences Center (Houston, TX).

Electron Microscopy of Nematode Cross Sections

CB286 nematodes grown at 15 or 25°C were washed off the plates with 3% glutaraldehyde in 0.1 M sodium phosphate (pH 7.4) and fixed for 3–4 h at 0°C. The rest of the procedure was carried as described (Mackenzie, et al., 1978).

Immunoblots

Equivalent amounts of similarly staged CB286 worms grown at 15 or 25°C were placed in SDS-β-mercaptoethanol buffer (Garcea et al., 1978), heated at 95°C for 5 min and vortexed. The samples were then centrifuged at 16,000 g for 5 min and the supernatants collected and kept at 0°C. The supernatants were run on 4.5% SDS-PAGE (Mini-Protean II system; Bio-Rad Laboratories, Hercules, CA; 100 V for 100 min) and transferred (Mini Trans-Blot system; Bio-Rad, Laboratories; 100 V for 120 min) to an Immobilon-NC membrane (Millipore Corporation, Bedford, MA). The membrane was blocked with 3% BSA in Tris-buffered saline + Tween 20 buffer (TBST: 50 mM Tris-HCl, 150 mM NaCl, 0.05% Tween 20, pH 7.6) for 1 h at room temperature and reacted simultaneously with isoform specific mAbs 5-23 (Epstein et al., 1985; anti-paramyosin, at 5 μg/ml in 3% BSA-TBST) and 28.2 (anti-mhc B, at 5 μg/ml in 3% BSA-TBST) for 1 h at room temperature. The reactions were detected using the ECL Western blotting analysis system (Amersham, Little Chalfont, Buckinghamshire, UK), using a 1:10,000 dilution of the provided peroxidase-labeled anti-mouse antibody, according to the manufacturer's instructions. The membrane was exposed for 30 s. The bands were quantitated using a Bio-Rad model 620 videodensitometer (Bio-Rad Laboratories). A second SDS-PAGE was performed, loading corrected volumes of supernatants in order to obtain equivalent optical densities for the bands corresponding to the anti-paramyosin reaction. The above procedure was followed for the preparation of the second membrane, with the addition of an antibody stripping step (1 h at 70°C in 100 mM β-mercaptoethanol, 2% SDS, 62.5 mM Tris-HCl, pH 6.7) followed by simultaneous reaction with monoclonal antibodies 5-23 (at 5 μg/ml in 3% BSA-TBST) and 5-6 (anti-mhc A at 2 μg/ml in 3% BSA-TBST; Miller et al., 1983), followed by detection and quantitation using the above procedure.

For analysis of protein from nematodes homogenized with Triton X-100, samples from the first tritonized fraction of the thick filament isolation procedure were used (Deitiker and Epstein, 1993). For analysis of soluble myosin heavy chain or paramyosin, samples were taken from the supernatants after centrifugation of the first tritonized fraction. Equal amounts of total protein, measured by the Bradford method (Bradford, 1976; Bio-Rad Laboratories), were separated on a 4.5% SDS-PAGE and the above procedure followed for detection of mhc A, mhc B, and paramyosin.

Thick Filament Isolation

The thick filament isolation procedure was carried out as described previously (Deitiker and Epstein, 1993). Two volumes of O.C.T. (Miles, Ekhart, IN) were added to each volume of nematodes and mixed. The samples were then stored in liquid nitrogen. 3-ml equivalent aliquots from the CB286 strain grown at 15 or 25°C were processed in parallel, using the same freshly prepared solutions and incubation times. Storage conditions of isolated filaments before immunofluorescence or immunoelectron microscopy were identical: 0°C for a maximum of 24 h.

Immunofluorescence Microscopy of Isolated Filaments

Thick filament enriched fractions in isolation buffer (IB: 80 mM KCl, 10 mM MgCl$_2$, 1.0 mM EDTA, 5.2 mM K$_2$HPO$_4$, 1.5 mM KH$_2$PO$_4$, 5 mM ATP, 0.5 M sucrose, and 1 μg/ml of the following protease inhibitors: chymostatin, pepstatin, leupeptin, trypsin inhibitor, N-benzoyl-L-arginine ethyl ester and p-toluidinyl sulfonyl-L-arginine methyl ester, pH 6.33–6.42) from the CB286 strain grown at 15 or 25°C were processed simultaneously. They were placed on precleaned (0.5 M KOH, 50% ethanol) microscope slides and incubated at room temperature for 5 min, washed once with IB and then blocked by incubation with 50% goat serum (GS) in IB for 1 h at room temperature in a humidification chamber. They were washed once with IB (10 min). For analysis of myosin isoform distribution, they were double-labeled with rhodamine-conjugated mAb 5-6 (specific for mhc A) and fluorescein-conjugated mAb 5-8 (specific for mhc B; Miller et al., 1983) at 2 and 5 μg/ml, respectively, in 10% GS-IB for 2 h at 37°C in a humidification chamber. For analysis of paramyosin distribution, they were labeled with rhodamine-conjugated mAb 5-23 (specific for paramyosin) in 10% GS-IB for 2 h at 37°C in a humidification chamber. They were then washed three times with IB (10 min each), mounted in p-phenylenediamine solution (1 mg/ml in 90% glycerol/PBS [0.01 M PO$_4$, pH 7.4 in 0.15 M NaCl], pH adjusted to 8.0 with 0.5 M carbonate-bicarbonate buffer, pH 9.0), and sealed with nail polish. Immunofluorescence microscopy was carried out on a Zeiss Photomicroscope III (Carl Zeiss, Thornwood, NY). Fluorochrome emission was visualized individually, and in combination through a 61002 DAPI/FITC/Texas red filter set (Carl Zeiss) and captured on Fujifilm Provia 1600 ASA film (color micrographs) or Kodak TMAX p3200 film (black and white micrographs).

Immunoelectron Microscopy of Isolated Filaments

Filament enriched fractions from CB286 strains grown at 15 or 25°C were processed simultaneously. They were placed on glow-discharged FORM-VAR carbon-coated copper grids (Ted Pella Inc., Redding, CA), incubated for 2 min at room temperature and washed with IB. They were then reacted with the primary mAb 5-6 (specific for mhc A, at 2 μg/ml in IB) or 28.2 (specific for mhc B, at 10 μg/ml in IB) and incubated for 10 min at room temperature in a humidification chamber. They were then washed with IB once and the secondary antibody (goat anti–mouse IgG at 20 μg/ml in IB) was applied and incubated for 10 min at room temperature in a humidification chamber. They were then washed with 0.1 M ammonium acetate, negatively stained by incubation with 2% uranyl acetate (in water) for 15 s and blotted to dryness. Electron microscopy was carried out on a JEOL JEM 100CX microscope (JEOL; Tokyo, Japan) at 20,000 magnification.

Results

The UNC-45 Protein Is Predicted to Contain Three Distinct Regions

The *unc-45* gene was identified by phenotypic rescue experiments (ACeDB, The Genome Informatics Group, Accession: clone W10B10, D. Pilgrim, University of Alberta, Edmonton, Alberta, Canada) and is predicted to contain 11 exons (*C. elegans* Genome Sequencing Project, The Sanger Centre, Hinxton Hall, Cambridge, UK and the Washington University School of Medicine, St. Louis, MO; data available from GenBank/EMBL/DDBJ under accession number U29096). The predicted exon structure of the gene was verified by sequencing two partial cDNAs: clone yk44f2, which spans from part of exon 6 (starting at nucleotide 812) to the polyadenylation site, and a PCR product of exons 1 to 6. The full-length cDNA encodes a 961–amino acid residue protein. We searched the GenBank Database (National Center for Biotechnology Information) using the basic local alignment search tool (Altschul et al., 1990) with the predicted protein sequence as query to identify proteins with regions of similarity that might offer clues about the potential structure and mechanism of action of UNC-45.

The NH$_2$-terminal region contains three TPR motifs (Hirano et al., 1990; Sikorski et al., 1990; Goebl and Yanagida, 1991; Fig. 1). These motifs are present in a wide variety of proteins in tandem arrays, their number ranging

from 3 to 16. Each motif is composed of two antiparallel α-helices (Fig. 1, *A* and *B*, *boxes*), and adjacent motifs pack in an antiparallel fashion with respect to each other, so that they form a continuous α-helical array that serves as a protein–protein interaction module (Das et al., 1998). They are characterized by a canonical sequence pattern of small and large hydrophobic residues, which allows the α-helices to pack tightly to form the array, and share rather loose primary sequence similarity. Fig. 1 shows a multiple sequence alignment of UNC-45 with four other sequences from proteins that contain TPR domains composed of three motifs. The consensus pattern of small and large hydrophobic amino acids is indicated: arrows point to positions 8, 20, and 27 of each motif, occupied by small hydrophobic amino acids and asterisks point to positions 1, 4, 11, 12, 17, 21 24, 28, and 30, which typically contain large hydrophobic residues. As can be observed, each TPR motif of UNC-45 fits this consensus pattern, except for positions 21 of motif No. 1; 1, 10, and 21 of motif No. 2; and 10 and 11 of motif No. 3. (which account for only 16% of the positions in the consensus, in a pattern similar to the protein hTOM). The UNC-45 TPR domain is as similar (47%) to the TPR domain of hPP5 as human protein TPR domains are among themselves (e.g., TPR domains of hPP5 and hTOM are 43% similar). A five–amino acid residue insertion (DKALR) between TPR motifs 1 and 2 of UNC-45 is predicted to form a loop between the two adjoining α-helices (SwissModel program; Guex and Peitsch, 1997) and

may provide specificity for interaction with partner proteins.

The COOH-terminal half of the molecule (amino acid residues 524 to 927, CRO1/She4p-like domain, Fig. 2) shows similarity to a region that spans roughly the COOH-terminal three-fifths of the fungal proteins CRO1 and She4p, which function in the differential segregation of molecules in distinct cellular processes. Our analysis of previously published pairwise alignments of these two proteins (Berteaux-Lecellier et al., 1998) showed that the region that is similar to UNC-45 (amino acid residues 270–678 of CRO1 and 336–773 of She4p, region 2) actually displays a better alignment than their NH$_2$-terminal two fifths (region 1). The identity for both regions is the same (20%), but region 2 has fewer gaps (8 vs. 12 in region 1), and these are much shorter (24 spaces present in gaps in region 2 vs. 121 in region 1), in spite of the fact that region 2 is considerably longer (three-fifths of the molecule). Our analysis of these sequences (Fig. 2) showed that region 2 of CRO1 is more similar to the CRO1/She4p-like domain of UNC-45 than to region 2 of She4p (25 vs. 20% identical; 36.2 vs. 31.5% similar). Region 2 of She4p is 18% identical and 28% similar to the UNC-45 CRO1/She4p-like domain. Several observations make our multiple sequence analysis result robust, even though the identity and similarity values of the pairwise comparisons by themselves may not appear highly significant. First, the presence of only 84 gap spaces within a total of 1,249 amino acid residue positions in the entire alignment is very low. The recurrence of regions of similarity in the three proteins suggests that this event is not due to chance (Altschul and
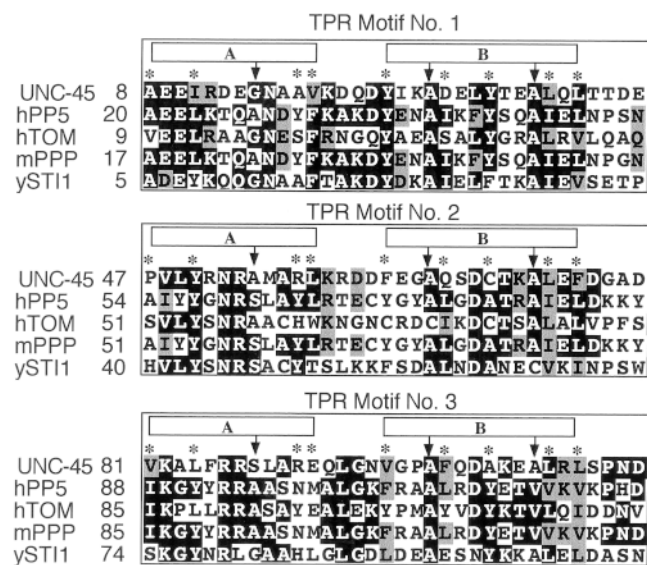

Figure 1. Multiple sequence alignments on which the UNC-45 TPR domain designation is based. The UNC-45 NH$_2$-terminal sequence is aligned with four other TPR-containing sequences. Identical residues have a black background; residues closely similar in charge or polarity, a gray one. Boxes *A* and *B* represent the anti-parallel α-helices of each motif. Consensus positions are indicated by arrows (small hydrophobic amino acid residues) and asterisks (large hydrophobic amino acid residues). Proteins listed are hPP5, human protein phosphatase 5 (U25174); hTOM, human putative outer mitochondrial membrane 34-kD translocase (U58970); mPPP, *Mus musculus* phosphoprotein phosphatase (U12204); ySTI1, *Saccharomyces cerevisiae* heat shock protein 1 (M28486).
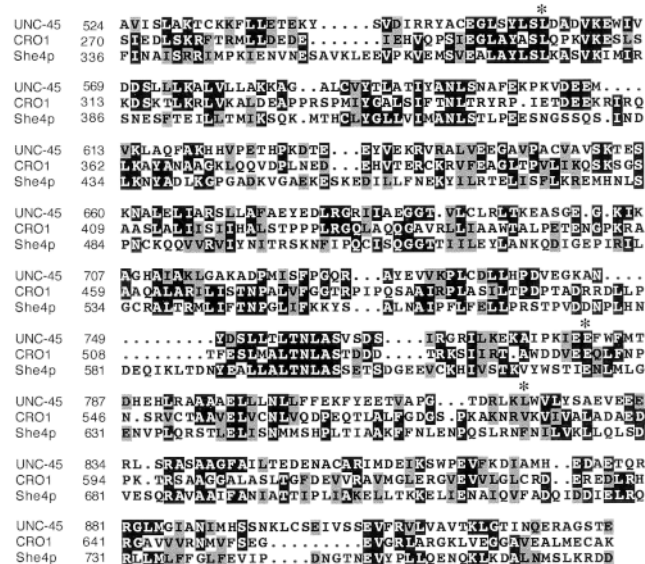

Figure 2. Multiple sequence alignments on which the UNC-45 CRO1/She4p-like domain designation is based. The UNC-45 COOH-terminal half is aligned with region 2 (see text) of the two related proteins CRO1 (Y16261), from *Podospora anserina*, and She4p (X93598), from *Saccharomyces cerevisiae*. Identical residues have a black background; residues closely similar in charge or polarity, a gray one. Asterisks indicate positions where mutations were found.

Table I. Sequence Alterations of unc-45 Alleles

Allele[*]	Detected by[‡]	Nucleotide substitution	Amino acid substitution
st603 (let)	HA	C628T	R210STOP
st601 (let)	HA	G1005A	W335STOP
b131 (ts)	HA	G1280A	G427E
su2002 (ts)	OT	T1676C	L559S
m94 (ts)	HA	G2341A	E781K
r450 (ts)	HA	G2341A	E781K
e286 (ts)	HA	C2464T	L822F

[*]let, Lethal allele; ts, temperature sensitive allele.
[‡]HA, hydroxylamine modification; OT, osmium tetroxide modification.

Lipman, 1990). Also, as shown below, this alignment is most consistent with our mutational analysis. The above observations allow us to propose that in these three proteins, the sequences shown in Fig. 2 form a domain that is separate from the rest of the molecule.

A region of 409 amino acid residues located between the TPR and CRO1/She4p-like domains of UNC-45 displays no significant similarity to any known protein. We have termed this region the central region of UNC-45.

The results of our sequence analysis suggest that the UNC-45 protein may contain three structurally different and possibly functionally distinct regions: TPR, central, and CRO1/She4p-like.

Different Phenotypic Classes of unc-45 Alleles Result from Mutations Localized to Distinct Predicted Regions

We decided to characterize the mutations responsible for the different types of unc-45 alleles in order to identify regions of the molecule that might be critical for its wild-type function. The CCM method was chosen to locate these mutations because it provided an effective alternative to direct sequencing of each allele, considering the size of the unc-45 gene (11 kbp without the promoter region). CCM allows efficient screening of multiple alleles simultaneously, in a stepwise manner (Cotton et al., 1988). Once a mutation was located in a particular allele, the segment where the mutation resided was sequenced.

After screening all exons for every allele, the following segments showed chemical cleavage: (a) following hydroxylamine treatment: exon 6 (alleles st603 and st601), exon 7 (allele b131), exon 9 (alleles m94 and r450), and exon 10 (allele e286); (b) following osmium tetroxide treatment: exon 8 (allele su2002). The procedure was repeated, to discard random mutations introduced by PCR, and these products were then sequenced. A single nucleotide substitution was found in each case (see Table I). All mutations were in agreement with (a) their predicted location in the PCR product according to the observed size of the cleavage product and (b) the type of substitution detected by each reaction: G/C to N for hydroxylamine and A/T to N for osmium tetroxide. Alleles m94 and r450 were found to contain identical nucleotide substitutions, which abolished an EcoRI recognition site. The identity of this mutation was further confirmed by the inability of this enzyme to digest exon 9 PCR products amplified from genomic DNA of both strains newly ordered from the Caenorhabditis Genetics Center (University of Minnesota, St. Paul, MN), and its ability to digest exon 9 PCR products amplified from N2 and e286 genomic DNA.

Analysis of the location of these mutations with respect to the predicted structure of the molecule (Figs. 2 and 8; Table I) showed that distinct types of alleles are located in particular regions of the molecule. Three of the four ts mutations (su2002, m94 = r450, and e286) were located in the CRO1/She4p-like domain. They were caused by missense substitutions in codons that encode residues conserved in the three proteins. A fourth ts allele (b131) was found in the central region, 97 codons upstream of the CRO1/She4p-like domain. The mutations responsible for the let alleles were substitutions that produced stop codons and thereby led to premature chain termination. In these cases, the CRO1/She4p-like domain could not be expressed. The results of our mutation analysis provide further evidence of the genomic sequence as that of the unc-45 locus and confirm the validity of the predicted reading frame.

Accumulation of Thick Filaments and mhc B, but Not mhc A, Is Decreased in the CB286 Strain Grown at 25°C

Previous work shows myofibrillar disorganization in the ts strain CB286 grown at the restrictive temperature (Epstein and Thomson, 1974). This sarcomeric defect is similar to the one observed in the mhc B null strain (Epstein et al., 1974) and is consistent with impaired assembly of thick filaments. To quantify the accumulation of thick filaments in this strain at either the permissive or the restrictive temperature, we compared equivalent anatomical zones (region II, which lies immediately posterior to the pharynx; Mackenzie et al., 1978). We counted the number of structures with diameters compatible with thick filaments in electron micrographs of transverse sections through the body wall muscles (Fig. 3). As can be observed, the strain grown at 15°C contained sarcomeres indistinguishable from wild-type (Fig. 3 a). However, the strain grown at 25°C produced disorganized myofibrillar structures such that individual sarcomeres could not be clearly delineated (Fig. 3 b). Therefore, the counts were performed on areas of equivalent dimensions, which cor-
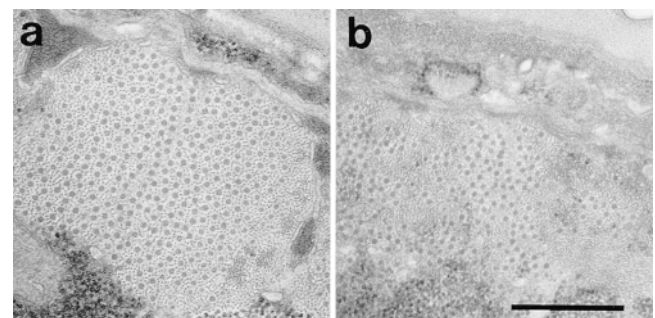

Figure 3. Thick filament accumulation in strain CB286 at 15 vs. 25°C. Electron micrographs of region II cross sections (Mackenzie et al., 1978) from nematodes grown at 15° (a) or 25°C (b). Bar, 0.5 mm.

responded to that occupied by a wild-type sarcomere. The 15°C sections had an average count of 359 filaments (values ranging from 331 to 395) and the 25°C had an average count of 197 filaments (values ranging from 117 to 270). Although the decrease in filament number in the strain grown at the restrictive temperature is clear (average of 45%), there is a greater variability from section to section. Several factors may contribute to this finding. The filaments may not all be aligned in the same orientation, or there may be populations of significantly shorter filaments. Both situations would lead to some micrographs showing considerably low filament counts, even though their actual number in the nematode may not be so decreased.

Since the phenotype described above is similar to the mhc B null, we decided to analyze the total accumulation of body wall mhc isoforms by immunoblotting. Total protein homogenates from populations of CB286 nematodes grown at the restrictive or permissive temperatures similarly staged (young adult) were transferred to a nitrocellulose membrane and probed with mhc isoform-specific mAbs (Fig. 4). First, the membrane was reacted with a mixture of mAbs 28.2 (anti-mhc B) and 5-23 (anti-paramyosin), and the reactions detected *via* chemiluminescence (Fig. 4 *b*). Then, the same membrane was stripped and reacted with mAbs 5-6 (anti-mhc A) and 5-23 (anti-paramyosin) and the reactions again detected by chemiluminescence (Fig. 4 *a*). The optical density of the reactions corresponding to paramyosin is very similar for both lanes in both experiments (Fig. 4 *a*: CB286 at 15°C = 0.164, CB286 at 25°C = 0.188; Fig. 4 *b*: CB286 at 15°C = 0.125, CB286 at 25°C = 0.141). These values confirm equal protein loading in both lanes and serve as an internal control for the comparisons of the accumulation of the mhc isoforms. The optical density of the reactions corresponding to mhc A was similar in both lanes (Fig. 4 *a*: CB286 at 15°C = 0.571, CB286 at 25°C = 0.633). However, the optical density of the reaction corresponding to mhc B in the 25°C CB286 sample was reduced by ~50% when compared with the sample from the 15°C strain: CB286 at 15°C = 0.609; CB286 at 25°C = 0.305 (Fig. 4 *b*). An independent experiment using samples of nematodes homogenized with the detergent Triton X-100 was in agreement with
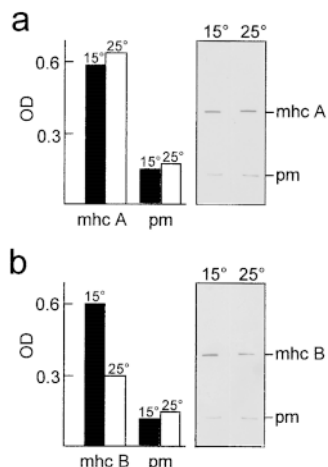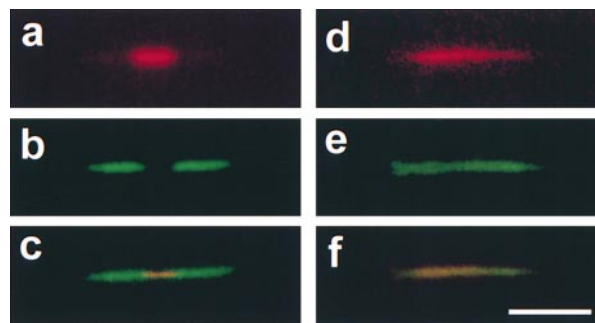

Figure 5. Immunofluorescence microscopy of myosin isoform distribution in strain CB286. Thick filaments isolated from nematodes grown at 15° (*a–c*) or 25°C (*d–f*) were reacted simultaneously with rhodamine-conjugated mAb 5-6 (specific for mhc A) and fluorescein-conjugated mAb 5-8 (specific for mhc B). (*a* and *d*) Rhodamine emission; (*b* and *e*) fluorescein emission; (*c* and *f*) simultaneous emission of both fluorochromes. Bar, 5 μm.

these results. It also showed us that none of the mhc isoforms or paramyosin were present as soluble material in samples from CB286 nematodes grown at either temperature.

Myosin Heavy Chain Isoforms Become Scrambled in Strain CB286 at the Restrictive Temperature

Our next set of experiments was designed to examine the structural characteristics of filaments isolated from CB286 worms grown at 15 or 25°C. For this purpose, thick filament enriched fractions were examined by immunofluorescence microscopy. Samples were reacted simultaneously with specific anti-isoform mAbs directly conjugated with either rhodamine (anti-mhc A antibody) or fluorescein (anti-mhc B antibody; Fig. 5). Thick filaments isolated from the 15°C strain revealed a myosin isoform distribution indistinguishable from that of wild-type. When analyzing rhodamine emission by itself (Fig. 5 *a*), a zone of ~1/4 to 1/5 the total length of the filament was observed, which corresponds to the central myosin A region. The fluorescein emission (Fig. 5 *b*) was excluded from this central region, but present in the rest of the filament, creating a central gap characteristic of myosin B localization. Simultaneous observation of both emissions (Fig. 5 *c*) revealed two yellow points at either side of the central region, which correspond to zones of overlap of both myosin isoforms, since co-localization of both fluorochromes is observed as a gold-colored emission. In contrast to these findings, the filaments isolated from the 25°C CB286 strain displayed a markedly abnormal distribution of myosin isoforms. The rhodamine emission (Fig. 5 *d*) revealed a myosin A distribution encompassing the entire observable length of most filaments. The fluorescein emission (Fig. 5 *e*) was also continuous throughout the filament, with no apparent gap in the center, indicating that myosin B was now also present in the central region of the filament. Simultaneous observation of both fluorochromes (Fig. 5 *f*) showed filaments that were entirely yellow, confirming the myosin isoform overlap throughout the filament. Similar analyses with mAb 5-23, specific for paramyosin, showed

Figure 4. mhc and paramyosin accumulation in strain CB286 at 15 vs. 25°C. Immunoblot of mhc A (*a*) and mhc B (*b*) content using paramyosin (*pm*) as an internal control. The same membrane was used in both experiments. The black (*15°C*) and white (*25°C*) bars represent the OD readings from the corresponding bands shown.

that filaments from CB286 grown at either temperature contain paramyosin throughout their lengths (data not shown). These results indicate that the differential localization of the myosin isoforms has been lost in filaments isolated from the CB286 strain grown at the restrictive temperature.

Because the result of immunofluorescence microscopy did not allow us to be certain that the structures being analyzed corresponded to single filaments, nor provided ultrastructural details, we examined individual filaments complexed with isoform-specific mAbs by electron microscopy. Isolated filaments were reacted independently with mAbs 5-6 and 28.2 and then an anti-mouse secondary antibody before being negatively stained (Fig. 6). Antibody reaction in electron micrographs of isolated filaments can be visualized as a continuous layer of additional protein complexes surrounding the filaments. It is especially evident when compared with unlabeled filaments (Fig. 6, *a* and *a'*). In filaments that contained zones of presence and absence of antibodies, a gradient of decreased labeling was observed as the reactions approached the regions devoid of antibodies. Boundaries between labeled and nonlabeled regions were clearly observed as transitions in the content of antibody complexes when observed at higher magnification (Fig. 6, *b'*, *d'*, and *e'*).

Thick filaments from the 15°C CB286 strain reacted with the mAbs in a pattern indistinguishable from that of wild-type, whereas their 25°C counterparts reacted in the abnormal manner consistent with the immunofluorescence microscopy experiments. Fig. 6, *a*–*c* show micrographs of lower magnification that allow comparison of the extent of the anti-mhc A reaction at either tempera-

ture. In the 15°C filaments, anti-mhc A reaction was observed only in the central 2-μm-long region of the filament (Fig. 6 *b*, inside the *arrowheads*), while the 25°C filaments reacted throughout their length (Fig. 6 *c*). Higher magnification showed the labeling transition in the 15°C filament (Fig. 6 *b'*) from the polar region devoid of anti-mhc A reaction to the central region recognized by this antibody; whereas it demonstrates the continuity of the reaction in the case of the 25°C filament (compare Fig. 6, *a'*–*c'*).

Fig. 6, *a*, *d*, and *e* demonstrate the extent of the anti-mhc B reactions at lower magnification. Filaments isolated from the strain grown at 15°C displayed the wild-type distribution of anti-mhc B labeling: reaction present in the polar regions but excluded from a 0.7-μm-long gap at the center (Fig. 6 *d*, outside the *arrowheads*). In contrast to this distribution, the anti-mhc B reaction entered the central region of the 25°C filaments: the anti-mhc B reaction occurred throughout most of the length of the filament (Fig. 6 *e*, outside the *arrowheads*), so that the gap was drastically shortened to as small as 0.3 μm. Higher magnification allowed visualization of the transitions in the reaction from the polar regions into the central region devoid of antibody (compare Fig. 6, *a'*, *d'*, and *e'*). The extent of the anti-mhc B reaction in the 25°C filaments indicates the rods of myosin B, in addition to those of myosin A, must be contributing to the anti-parallel interactions of the central bare zone. This situation is similar to that observed in filaments isolated from paramyosin loss-of-function worms, where myosin isoforms A and B scramble in the central region of the filament (Epstein et al., 1986).

During our electron microscopy analysis, we also noticed that >50% of the filaments had areas devoid of myosin at their ends, where core structures could be observed. This is in agreement with our immunofluorescence microscopy observation that filaments from the 25°C CB286 strain contain paramyosin.

Taking into account the lower resolution of immunofluorescence microscopy, which was unable to detect the short area devoid of anti-mhc B reaction, the immunoelectron microscopy results confirmed the optical microscopy observations. They demonstrated that scrambling of the myosin isoforms occurred in filaments isolated from the CB286 strain grown at 25°C, and that these filaments contain paramyosin core structures.

Thick Filaments Assembled In Vivo in Strain CB286 at the Restrictive Temperature Are Unstable In Vitro

Apart from the myosin localization defect discussed above, thick filaments isolated from the CB286 strain grown at the restrictive temperature also displayed abnormally low yields after the isolation procedure, as well as reduced length.

Thick filaments were isolated simultaneously from equivalent amounts of similarly staged populations of CB286 worms grown at 15 or 25°C. However, as evidenced by immunofluorescence microscopy, the yield of thick filaments from the mutant strain grown at 25°C (Fig. 7 *b*) was drastically lower than its 15°C counterpart, (Fig. 7 *a*). To obtain fields with similar filament densities, the fractions of filaments from the 15°C specimens needed to be diluted 1:250 to 1:500. This decrease in yield was confirmed during the
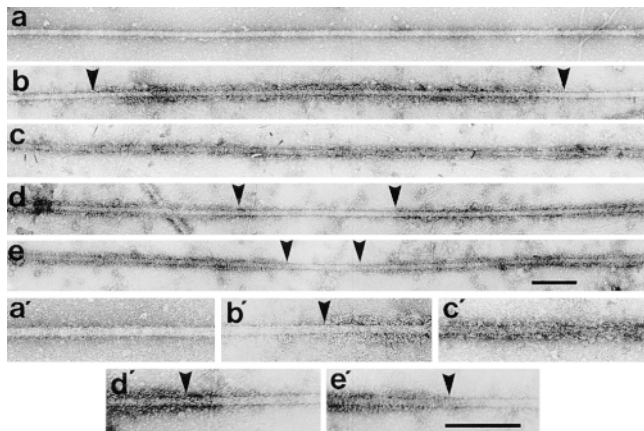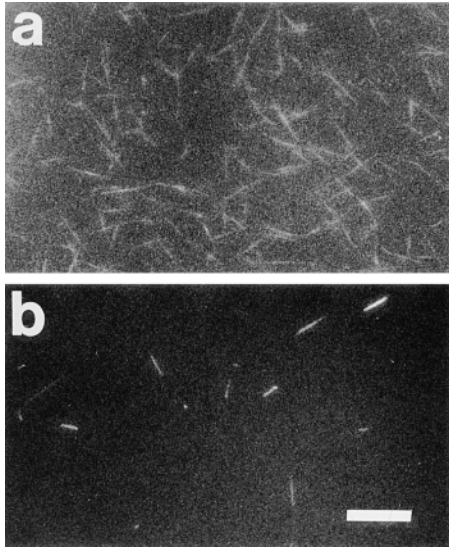

Figure 6. Immunoelectron microscopy of myosin isoform distribution in strain CB286. (*a*) Negatively stained 15°C filament; (*b*) mAb 5-6 (mhc A specific) labeling of 15°C filament, reaction can be seen inside arrowheads; (*c*) mAb 5-6 labeling of 25°C filament, reaction can be seen throughout its length; (*d*) mAb 28.2 (mhc B specific) labeling of 15°C filament, reaction can be seen outside arrowheads; (*e*) mAb 28.2 labeling of 25°C filament, reaction can be seen outside arrowheads. Zones of interest in *a* through *e* can be observed at higher magnification in *a'* through *e'*, respectively, and show the presence (*b'*, *d'*, and *e'*) or absence (*a'* and *c'*) of labeling transitions due to reacting and nonreacting regions along individual filaments. *a'* is unreacted and *c'* is labeled homogeneously by anti-mhc A antibody. Bars: (*a–e* and *a'–e'*) 0.2 μm.

Figure 7. Immunofluorescence microscopy of thick filament isolation in strain CB286. Undiluted samples of 6.2 K supernatant thick filament enriched fractions (Deitiker and Epstein, 1993) from equivalent amounts of starting materials from nematodes grown at 15 or 25°C were reacted simultaneously with rhodamine-conjugated mAb 5-6 (specific for mhc A) and fluorescein-conjugated mAb 5-8 (specific for mhc B). (*a*) Simultaneous emission of both fluorochromes in 15°C sample; (*b*) simultaneous emission of both fluorochromes in 25°C sample. Bar, 10 μm.

electron microscopy analysis. This marked reduction of isolated filament number contrasts with only a 30–70% reduction observed in vivo. An explanation for this difference may be decreased stability of the filaments in the strain grown at 25°C.

Individual lengths of negatively stained isolated filaments from 15 or 25°C CB286 worms were measured. The average 15°C filament length was 5.87 μm ($n = 90$; $s = 4.41$), while the average 25°C filament length was 3.47 μm ($n = 90$; $s = 2.25$). This difference was found to be statistically significant, as judged by the *t* test: $t(178) = 9.79$, $P < 0.0001$.

The marked reduction of filament length and number upon isolation beyond what was observed in the corresponding electron microscopy cross-sections from 25°C CB286 nematodes was most likely the result of filament disassembly during the isolation procedure. If the filaments were only being mechanically sheared because of increased fragility, the number of structures observed would be substantially increased. Each filament that breaks would produce at least two shorter fragments. This was not the case, and therefore we propose that thick filaments isolated from CB286 nematodes grown at the restrictive temperature underwent enhanced in vitro depolymerization.

Discussion

The predicted UNC-45 sequence contains three distinct regions: an NH$_2$-terminal TPR domain, a central region with no significant similarity to any known protein, and a COOH-terminal CRO1/She4p-like domain. This last region is the target of three of the four *ts* mutations analyzed, which are caused by base substitutions leading to missense mutations in codons for conserved residues (Fig. 8). The two lethal alleles studied are the result of base substitutions in the central region, which lead to premature chain termination, so that the CRO1/She4p-like domain cannot be expressed.

This work has also provided discrete evidence of abnormal structure in *unc-45* mutant thick filaments. Comparison of thick filaments from the CB286 strain grown at the restrictive versus the permissive temperature has demonstrated that this *ts* mutation, located within the CRO1/She4p-like domain, affects the accumulation of assembled thick filaments, as well as their myosin isoform distribution and in vitro stability.

The results presented here suggest that UNC-45 functions as a thick filament assemblase through its CRO1/She4p-like domain. Assemblase activity may be defined as a catalyst or chaperone that mediates the incorporation of myosin and related proteins into thick filaments (Liu et al., 1997). Several mechanisms may be involved, including catalysis of myosin folding at the ribosome, intracellular myosin transport, posttranslational modification of myosin and associated proteins, catalysis of myosin polymerization, sorting of myosin isoforms, and scaffolding of myosin, paramyosin and the filagenins during the actual formation of the filament. An assemblase molecule may participate in one or more of these processes as a catalyst and may be subject to regulation by the interaction of additional proteins.

The scrambling of myosins A and B in the central region of 25°C CB286 filaments indicates that both isoforms contribute to the anti-parallel interactions of the central region of the filament, as has been demonstrated to be the case in filaments isolated from paramyosin loss-of-function mutant nematodes (Epstein et al., 1986). Therefore, additional factors are necessary to recognize these isoforms and place them differentially along the length of the filament. One probable function of UNC-45 may be to sort each myosin isoform during the assembly process. This model of directed assembly of muscle thick filaments proposes that additional processes and specific proteins are required to explain the behavior of myosin besides its simple self-assembly as discussed by McLachlan and Karn (1982) and Hoppe and Waterston (1996).

Several independent lines of evidence support the requirement for additional functions during the construction of thick filaments. In *Drosophila melanogaster*, a single mhc gene is alternatively spliced to produce different iso-
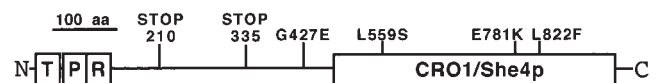

Figure 8. Model of UNC-45 predicted structure. The TPR and CRO1/She4p-like domains are represented by boxes; the central region, with no similarities to any known protein, by a horizontal line connecting the boxes. The positions of the mutant amino acid substitutions identified are indicated by vertical lines. Putative functions of each region are discussed in the text.

forms that assemble into thick filaments of different characteristics, depending on the tissue and developmental stage of the organism (Bernstein et al., 1983). Transgenic flies that express only a single mhc isoform, however, are still able to assemble different types of thick filaments with characteristics appropriate to the tissue and developmental stage (Wells et al., 1996). Additional factors must then enable this single myosin species to assemble into distinct structures. In *C. elegans* body wall muscle cells, thick filament length varies according to the developmental stage of the organism. Embryonic filaments cannot be longer than the greatest dimension of the embryonic muscle cell (<5 μm; Epstein et al., 1993), whereas adult thick filaments are 9.7 μm long (Mackenzie and Epstein, 1980). There must be factors that regulate filament elongation according to the developmental stage of the muscle cell other than myosins A and B and paramyosin, which are present continously. Moreover, myosins from different species that assemble in vivo into filaments of different characteristics (Epstein, 1989) form very similar filamentous structures under the same conditions in vitro (Harris and Epstein, 1977). Also, mutant CB675 myosin, which disrupts thick filament assembly in vivo, forms indistinguishable filamentous structures from those formed by wild-type molecules under the same conditions in vitro (Harris and Epstein, 1977). This indicates that myosin molecules must be interacting with additional factors in vivo that regulate their proper assembly into thick filaments. Three-dimensional structural work on nematode thick filament cores has shown that these consist of paramyosin subfilaments held together in a tubular arrangement by additional protein structures (Epstein et al., 1995). Several of these proteins have now been identified, including β-filagenin (Liu et al., 1998), and their role as cross-linking proteins demonstrates the presence of additional proteins involved in the assembly of myosin filaments.

One possible role for the TPR domain of UNC-45 may be to bring interacting proteins to the site of thick filament assembly. These may be proteins that are additional components of the proposed assemblase, which contribute their particular functions during the assembly process, including protein chaperones, prolyl isomerases, and phosphoprotein phosphatases. Other partner proteins brought to the site of filament assembly through TPR binding may provide regulatory properties on the assemblase, appropriate to tissue and developmental stage of thick filament construction. We currently have no information as to the functional role the central region. It may be involved in an assemblase activity because one of the *ts* mutations is localized within its boundaries. The multi-domain nature of UNC-45 (Fig. 8) suggests that each region may specifically interact with different kinds of protein molecules and perhaps act at distinct steps during thick filament assembly.

Several observations suggest that the actual process of thick filament assembly rather than the stability of the UNC-45 protein or the filaments themselves may be sensitive to elevated temperature in the *unc-45 ts* alleles. A significant loss of UNC-45 function leads to lethality (Venolia and Waterston, 1990). Therefore, the *ts* mutations cannot cause complete misfolding of UNC-45 at the restrictive temperature; a partial function (or set of func-

tions) must be present to allow survival of the organism. Also, our finding that three *ts* alleles are caused by mutations in residues conserved in UNC-45, CRO1, and She4p suggests that these residues may represent key interactions in the UNC-45 active site and that their substitution causes specific defects rather than destabilization of the protein. Furthermore, there is genetic evidence that the protein product of the *ts* alleles is not wild-type at the permissive temperature (Venolia and Waterston, 1990); the *mr/mr* progeny of a *mr/ts* hermaphrodite are F_1 lethals at either 15 or 25°C, whereas the *mr/mr* progeny of a *mr/+* hermaphrodite are viable and produce mostly F_2 lethals. A plausible interpretation of these interallelic interactions is that the UNC-45 protein may work as an oligomer, and the presence of a *ts* protein, even at 15°C, hinders UNC-45 activity. It is unlikely that the thick filaments are sensitive to the elevated temperature because adult nematodes from any of the *ts* strains grown at the permissive temperature do not show phenotypic reversal when switched to 25°C. This indicates that the myofibrils in these worms are stable structures not susceptible to depolymerization due to increased temperature.

Our results on the accumulation of mhc isoforms in the CB286 strain grown at 15 versus 25°C suggest that this mutation, localized within the CRO1/She4p-like domain, may affect the dynamics of myosin B polymerization. Work by others (Bejsovec and Anderson, 1990) has demonstrated that dominant lethal mutations in the myosin B head lead to impaired filament assembly and decreased accumulation of myosin B. A plausible interpretation of these results is that the mutations cause misfolding of the myosin molecule, which in turn hinders the thick filament assembly process. The presumably misfolded myosin B is then degraded. A similar situation may be occurring in CB286 nematodes at 25°C. A defect of UNC-45 function may lead to an abnormal myosin B, which then causes an impairment of filament assembly reflected by reduced numbers of filaments assembled in vivo, scrambling of myosin isoforms, and in vitro filament depolymerization. The decreased accumulation of myosin B may be explained by increased degradation of unincorporated molecules. Alternatively, the CB286 defect may cause a reduced number of functional myosin B molecules to be available for assembly. This could explain the similarity with the mhc B null phenotype observed in cross-sections by electron microscopy, and the decreased accumulation of mhc B. The yeast protein She4p may play a similar role to UNC-45 during the assembly of Myo4p (She1p) into structures capable of transporting the repressor Ahs1p. A common substrate of both molecules may be the myosin head, since this domain is conserved in both unconventional and sarcomeric myosins (Cheney and Mooseker, 1992).

An alternative, but unlikely, explanation for the observed myosin isoform scrambling in the 25°C CB286 strain could be myosin repolymerization in vitro. Our data indicated that there was substantial filament depolymerization during the isolation procedure. Some of the myosin molecules could have dissociated from the filament and reassembled in a disorganized fashion in vitro to produce the abnormal structures observed by immunofluorescence and immunoelectron microscopy. If these structures originally had a myosin isoform distribution similar to wild-

type in vivo, they would contain a central myosin A region. It has been shown that this myosin isoform remains tightly associated with the filament until the paramyosin core itself depolymerizes (Deitiker and Epstein, 1993). Because the 25°C filaments contained paramyosin cores, which always retain myosin A in vitro, it appears unlikely that myosin A could have dissociated and then repolymerized with myosin B along nearly the entire length of the thick filament, including the central zone.

Biochemical investigation of the potential physical interactions between UNC-45 and the myosin isoforms is required in order to understand the mechanisms involved in its wild-type function(s). UNC-45 may associate with thick filament components in a stable fashion. In this case, it may act as part of a protein scaffold in the positioning of specific myosin isoforms and related proteins along the filament. As a scaffolding protein, UNC-45 may have additional nonstructural activities, in a manner analogous to twitchin, which is both a structural component of the sarcomere and a myosin light chain kinase (Hu et al., 1994; Lei et al., 1994) or the sarcomeric myosin itself, which is an ATPase, a protein motor and a structural protein (Harris and Epstein, 1977; Warrick and Spudich, 1987). In this case, the UNC-45 protein may be a structural component of the filament. On the other hand, involvement of UNC-45 in any of the other possible roles of a thick filament assemblase would require only transient association with filament components and not stable association with a particular sarcomeric structure.

The information related to myosin assembly presented here for UNC-45 suggests that UCS proteins (UNC-45/CRO1/She4p) may serve as components of protein machines that recognize specific myosin isoforms and localize them to subcellular sites, where they can be assembled into structures appropriate for their particular cellular function.

References

Altschul, S.F., and D.J. Lipman. 1990. Protein database searches for multiple alignments. *Proc. Natl. Acad. Sci. USA*. 87:5509–5513.

Altschul, S.F., W. Gish, W. Miller, E.W. Myers, and D.J. Lipman. 1990. Basic local alignment search tool. *J. Mol. Biol.* 215:403–410.

Barstead, R.J., and R.H. Waterston. 1991. Vinculin is essential for muscle function in the nematode. *J. Cell Biol.* 114:715–724.

Bernstein, S.I., K. Mogami, J.J. Donady, and C.P. Emerson, Jr. 1983. *Drosophila* muscle myosin heavy chain encoded by a single gene in a cluster of muscle mutations. *Nature*. 302:393–397.

Berteaux-Lecellier, V., D. Zickler, R. Debuchy, A. Panvier-Adoutte, C. Thompson-Coffe, and M. Picard. 1998. A homologue of the yeast *SHE4* gene is essential for the transition between the syncytial and cellular stages during sexual reproduction of the fungus *Podospora anserina*. *EMBO (Eur. Mol. Biol. Organ.) J.* 17:1248–1258.

Besjovec, A., and P. Anderson. 1990. Functions of the myosin ATP and actin binding sites are required for *C. elegans* thick filament assembly. *Cell*. 60:133–140.

Bradford, M.M. 1976. A rapid and sensitive method for the quantitation of microgram quantities of protein utilizing the principle of protein-dye binding. *Anal. Biochem.* 72:248–254.

Brenner, S. 1974. The genetics of *Caenorhabditis elegans*. *Genetics*. 77:71–94.

Cheney, R.E., and M.A. Mooseker. 1992. Unconventional myosins. *Curr. Opin. Cell Biol.* 4:27–35.

Cotton, R.G.H., N.R. Rodrigues, and R.D. Campbell. 1988. Reactivity of cytosine and thymine in single-base-pair mismatches with hydroxylamine and osmium tetroxide and its application to the study of mutations. *Proc. Natl. Acad. Sci. USA*. 85:4397–4401.

Das, A.K., P.T.W. Cohen, and D. Barford. 1998. The structure of the tetratricopeptide repeats of protein phosphatase 5: implications for TPR-mediated protein-protein interactions. *EMBO (Eur. Mol. Biol. Organ.) J.* 17:1192–1199.

Deitiker, P.R., and H.F. Epstein. 1993. Thick filament substructures in *Caenorhabditis elegans*: evidence for two populations of paramyosin. *J. Cell Biol.* 123:303–311.

Epstein, H.F., and J.N. Thomson. 1974. Temperature-sensitive mutation affecting myofilament assembly in *Caenorhabditis elegans*. *Nature*. 250:579–580.

Epstein, H.F., R.H. Waterston, and S. Brenner. 1974. A mutant affecting the heavy chain of myosin in *Caenorhabditis elegans*. *J. Mol. Biol.* 90:291–300.

Epstein, H.F., D.M. Miller, I. Ortiz, and G.C. Berliner. 1985. Myosin and paramyosin are organized about a newly identified core structure. *J. Cell Biol.* 100:904–915.

Epstein, H.F., I. Ortiz, and L.A. Traeger Mackinnon. 1986. The alteration of myosin isoform compartmentation in specific mutants of *Caenorhabditis elegans*. *J. Cell Biol.* 103:985–993.

Epstein, H.F. 1989. Modulation of myosin assembly. *In* Cellular and Molecular Biology of Muscle Development. L.H. Kedes, and F.A. Stockdale, editors. Alan R. Liss, Inc., N.Y. 207–219.

Epstein, H.F., D.L. Casey, and I. Ortiz. 1993. Myosin and paramyosin of *Caenorhabditis elegans* embryos assemble into nascent structures distinct from thick filaments and multi-filament assemblages. *J. Cell Biol.* 122:845–858.

Epstein, H.F., G.Y. Lu, P.R. Deitiker, I. Ortiz, and M.F. Schmid. 1995. Preliminary three-dimensional model for nematode thick filament core. *J. Struct. Biol.* 115:163–174.

Garcea, R.L., F. Schachat, and H.F. Epstein, 1978. Coordinate synthesis of two myosins in wild-type and mutant nematode muscle during larval development. *Cell*. 15:421–428.

Goebel, M., and M. Yanagida. 1991. The TPR snap helix: a novel protein repeat motif from mitosis to transcription. *Trends Biochem. Sci.* 16:173–177.

Guex, N., and M.C. Peitsch. 1997. SWISS-MODEL and the Swiss-PdbViewer: an environment for comparative protein modelling. *Electrophoresis*. 18:2714–2723.

Harris, H.E., and H.F. Epstein. 1977. Myosin and paramyosin of *Caenorhabditis elegans* biochemical and structural properties of wild-type and mutant proteins. *Cell*. 10:709–719.

Hirano, T., N. Kinoshita, K. Morikawa, and M. Yanagida. 1990. Snap helix with knobs and hole: essential repeats in *S. pombe* nuclear protein *nuc2+*. *Cell*. 60:319–328.

Hoppe, P.E., and R.H. Waterston. 1996. Hydrophobicity variations along the surface of the coiled-coil rod may mediate striated muscle myosin assembly in *Caenorhabditis elegans*. *J. Cell Biol.* 135:371–382.

Hu, S.H., M.W. Parker, J.Y. Lei, M.C. Wilce, G.M. Benian, and B.E. Kemp. 1994. Insights into autoregulation from the crystal structure of twitchin kinase. *Nature*. 369:581–584.

Jansen, R., C. Dowzer, C. Michaelis, M. Galova, and K. Nasmyth. 1996. Mother cell-specific *HO* expression in budding yeast depends on the unconventional myosin Myo4p and other cytoplasmic proteins. *Cell*. 84:687–697.

Lei, J., X. Tang, T.C. Chambers, J. Pohl, and G.M. Benian. 1994. Protein kinase domain of twitchin has protein kinase activity and an autoinhibitory region. *J. Biol. Chem.* 269:21078–21085.

Lewis, J.A., and J.T. Fleming. 1995. Basic Culture Methods. *In Caenorhabditis elegans*: Modern Biological Analysis of an Organism. H.F. Epstein and D.C. Shakes, editors. Academic Press, Inc., San Diego, CA. 3–29.

Liu, F., J.M. Barral, C.C. Bauer, I. Ortiz, R.G. Cook, M.F. Schmid, and H.F. Epstein. 1997. Assemblases and coupling proteins in thick filament assembly. *Cell Struct. Funct.* 22:155–162.

Liu, F., C.C. Bauer, I. Ortiz, R.G. Cook, M.F. Schmid, and H.F. Epstein. 1998. β-filagenin, a newly identified protein coassembling with myosin and paramyosin in *Caenorhabditis elegans*. *J. Cell Biol.* 140:347–353.

Mackenzie, J.M., R.L. Garcea, J.M. Zengel, and H.F. Epstein. 1978. Muscle development in *Caenorhabditis elegans*: mutants exhibiting retarded sarcomere construction. *Cell*. 15:751–762.

Mackenzie, J.M., and H.F. Epstein. 1980. Paramyosin is necessary for determination of nematode thick filament length *in vivo*. *Cell*. 22:747–755.

McLachlan, A.D., and J. Karn. 1982. Periodic charge distribution in the myosin rod amino acid sequence match cross-bridge spacings in muscle. *Nature*. 299:226–231.

Miller, D.M., I. Ortiz, G.C. Berliner, and H.F. Epstein. 1983. Differential localization of two myosins within nematode thick filaments. *Cell*. 34:477–490.

Sambrook, J., E.F. Fritsch, and T. Maniatis. 1989. Molecular Cloning A Laboratory Manual. Cold Spring Harbor Laboratory, Cold Spring Harbor, NY. E3–E4.

Schachat, F., R.L. Garcea, and H.F. Epstein. 1978. Myosins exist as ho-

modimers of heavy chains: demonstration with specific antibody purified by nematode mutant myosin affinity chromatography. *Cell.* 15:405–411.

Sikorski, R.S., M.S. Boguski, M. Goebl, and P. Hieter. 1990. A repeating amino acid motif in CDC23 defines a new family of proteins and a new relationship among genes required for mitosis and RNA synthesis. *Cell.* 60:319–328.

Smith, R.F., B.A. Wiese, M.K. Wojzynski, D.B. Davison, and K.C. Worley. 1996. BCM Search Launcher—an integrated interface to molecular biology data base search and analysis services on the world wide web. *Genome Res.* 6:454–462.

Venolia, L., and R.H. Waterston. 1990. The *unc-45* gene of *Caenorhabditis elegans* is an essential muscle-affecting gene with maternal expression. *Genetics.* 126:345–353.

Warrick, H.M., and J.A. Spudich. 1987. Myosin structure and function in cell motility. *Ann. Rev. Cell Biol.* 3:379–421.

Waterston, R.H. 1988. Muscle. *In* The Nematode *Caenorhabditis elegans*. W.B. Wood, editor. Cold Spring Harbor Laboratory, Cold Spring Harbor, NY. 281–335.

Waterston, R.H. 1989. The minor myosin heavy-chain, MHC A, of *Caenorhabditis elegans* is necessary for the initiation of thick filament assembly. *EMBO (Eur. Mol. Biol. Organ.) J.* 8:3429–3436.

Wells, L., K.A. Edwards, and S.I. Bernstein. 1996. Myosin heavy chain isoforms regulate muscle function but not myofibril assembly. *EMBO (Eur. Mol. Biol. Organ.) J.* 15:4454–4459.

Wendland, B., J.M. McCaffery, Q. Xiao, and S.D. Emr. 1996. A novel fluorescence-activated cell sorter-based screen for yeast endocytosis mutants identifies a yeast homologue of mammalian eps15. *J. Cell Biol.* 135:1485–1500.

Williams, B.D., and R.H. Waterston. 1994. Genes critical for muscle development and function in *Caenorhabditis elegans* identified through lethal mutations. *J. Cell Biol.* 124:475–490.